P1.3 Analysis of Surface Thermodynamic Characteristics within the Rear-Flank Downdraft of the Wichita, Kansas, Tornadic Supercell of 14 April 2012

KYLE YAFFE, ANDREW GORDON, AND JEFFREY FRAME

Department of Atmospheric Sciences, University of Illinois at Urbana-Champaign, Urbana, IL

1. Introduction

On 14 April 2012, a long-lived supercell moved across the Wichita, KS, metropolitan area and produced an EF-3 tornado, which tracked through southeast portions of the area (Fig. 1). This tornado touched down at approximately 0318 UTC, 1.5 km west of I-35 in Haysville, KS, and dissipated at approximately 0341 UTC, 1.5 km northwest of the I-35/K-96 junction in northeast Wichita (NWS Wichita 2012). This supercell initiated along a dryline over the northern Texas Panhandle, and had already produced several tornadoes by the time it entered the Wichita area around 0300 UTC.

Three Automated Surface Observing Systems (ASOS) – at McConnell Air Force Base (KIAB), Wichita Mid-Continent Airport (KICT), and Colonel James Jabara Airport (KAAO) – took high-resolution special METAR observations, with temporal density of up to one minute, as the supercell and tornado traversed the city. The supercell was also observed by the Wichita National Weather Service Weather Surveillance Radar 1988-Doppler (WSR-88D; KICT), and the tornado passed within 14 km of the radar site.

These surface data are significant because they permit a detailed analysis of the thermodynamic fields within the storm inflow, as well as within the forward-flank downdraft (FFD) and rear-flank downdraft (RFD) regions of the storm. Focus was placed upon the equivalent potential temperature (θ_e) and the virtual potential temperature (θ_v) fields in these regions in order to further justify the assertion that RFDs with relatively small deficits of θ_e and θ_v (i.e., relatively warmer and more potentially buoyant RFDs) are associated with a greater likelihood of long-lived and more intense tornadoes (e.g., Markowski et al. 2002; Shabbott and Markowski 2006; Grzych et al. 2007; Lee et al. 2011; Lee et al. 2012). The analysis of the pressure field will also allow the pressure deficit near the tornado to be quantified. The details of data collection and methodology are discussed within section 2, while section 3 presents the results. Conclusions and suggestions for future research can be found in section 4.

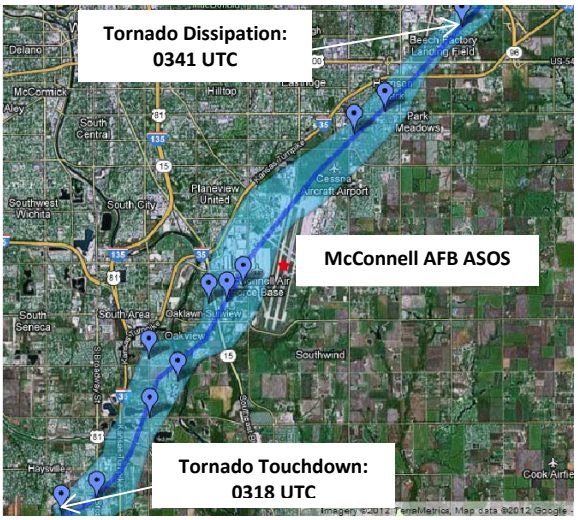

Figure 1. Map illustrating the tornado track (shaded in blue) and center line of the tornado track (heavy blue line). Location of the KIAB ASOS site is indicated by the red star. Map courtesy NWS Wichita (2012).

2. Data and methodology

METAR format surface observations from each observation site were obtained and decoded, and the latitude and longitude of each site were determined. Radar data from the KICT WSR-88D were also acquired and used to compute the storm motion over 12-minute intervals by tracking the low-level mesocyclone. The ASOS sites were then matched to their precise locations on the radar images and plotted using a simple time-to-space conversion and the computed storm motion vectors. Each radar image displays surface data collected over a 24-minute period centered on the time at which the radar image was recorded; it was assumed that the storm structure did not change significantly over this period of time. This method is similar to that employed by Markowski et al. (2002) and Grzych et al. (2007), except that the surface observing platforms were stationary in this case.

The computation of θ_e and the perturbation, θ_e', require the calculation of the equivalent temperature, T_e, which is given by

$$T_e = T + \left(\frac{L_v w}{c_p + w c_w} \right)$$

(Bohren and Albrecht, 1998, p. 285). In this equation, T is the air temperature in K, L_v is the latent heat of vaporization of liquid water (2.5 MJ kg^{-1}), w is the dimensionless water vapor mixing ratio, c_p is the specific heat capacity of dry air at constant pressure (1004 J kg^{-1} K^{-1}), and c_w is the specific heat of liquid water (4218 J kg^{-1} K^{-1}). From here, θ_e can be computed following

$$\theta_e = T_e \left(\frac{p_0}{p} \right)^{\frac{R_d}{c_p}}$$

where p_0 is the standard reference pressure (1000 mb), p is the environmental pressure, and R_d is the gas constant for dry air (287 J kg^{-1} K^{-1}).

The equivalent potential temperature perturbation, θ_e', was then found from $\theta_e' = \theta_e - \bar{\theta}_e$, in which $\bar{\theta}_e$ is the mean equivalent potential temperature of the prestorm environment. This was computed by averaging θ_e at all three surface observing stations from the METAR observations taken between 0153-0155 UTC. At this time, precipitation had not yet begun at any of the ASOS sites, and no outflow or other boundaries had contaminated the prestorm environment. Additionally, any error due to nocturnal cooling was mitigated by the presence of cloud cover and strong warm-air advection, but a small error on the order of 1 K is still possible given the temporal coarseness of the prestorm METAR data.

The computation of θ_v required the calculation of the potential temperature, θ, which is determined by

$$\theta = T \left(\frac{p_0}{p} \right)^{\frac{R_d}{c_p}}$$

From here, θ_v can be found utilizing $\theta_v = (1 + 0.61w)\theta$. The mean, $\bar{\theta}_v$, and the perturbation, θ_v', were then found with a method identical to that employed for $\bar{\theta}_e$ and θ_e' above.

0331 UTC

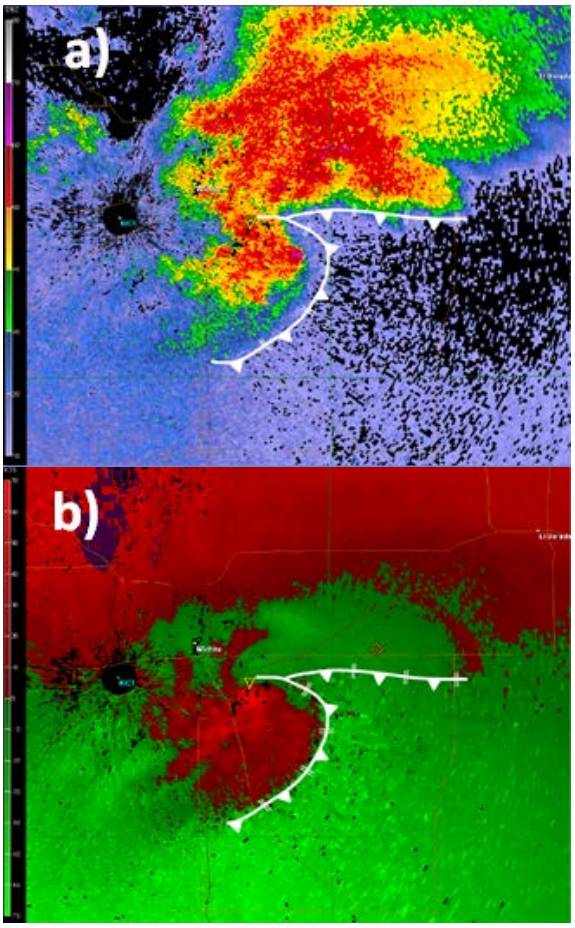

Figure 2. KICT 0.5º (a) reflectivity image and (b) radial velocity image at 0331 UTC with the locations of the forward-flank and rear-flank gust fronts indicated.

3. Results

When the supercell entered the Wichita area around 0300 UTC 15 April 2012, the forward flank of the storm displayed a sharp reflectivity gradient along its right (southern) flank, as well as a pronounced hook echo on the right-rear flank (Fig. 2a). The hook echo increased in size as the tornado progressed to the northeast through 0341 UTC. It then began decreasing in size and losing organization at 0350 UTC, and the hook echo dissipated completely around 0442 UTC about 40 km northeast of El Dorado (not shown).

Throughout the analysis period, southeasterly winds were present in the inflow southeast of the storm and within the southern portion of the forward flank, and southwesterly

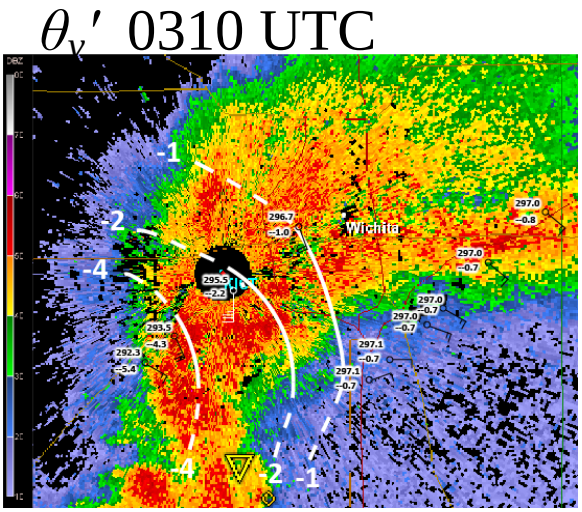

Figure 3. KICT reflectivity 0.5º image at 0310 UTC with θ_v observations superposed. On the station models, the top number is θ_v (K), the bottom number is θ_v' (K), and ground relative winds are also indicated (knots) with standard notation. Contour lines show θ_v', and the contour interval is 2 K, except that the -1 K contour is also shown. Contours are dashed in regions where their location is less certain. The yellow triangle shows the location of the radar-determined tornado vortex signature.

winds existed behind the rear-flank gust front (Figs. 2a and 2b). The forward-flank gust front extended nearly due eastward from the tornado position, and was marked by a slight wind shift near the southern edge of the forward-flank reflectivity core; winds south of the front were characterized by strong inbound velocities, with weaker inbound velocities to the north of this boundary. The rear-flank gust front extended southward, then southwestward from the tornado position. Its location was more easily determined, as there was a clear boundary between outbound radial velocities within the rear-flank outflow and inbound velocities within the inflow. Also note that the tornado had occluded by 0331 UTC.

An analysis of θ_v at 0310 UTC (Fig. 3) shows only small deficits, on the order of 1 K, within the forward flank, with larger deficits of 4-5 K near the left-rear flank of the storm. This analysis is consistent with that of Shabbott and Markowski (2006), who generally found smaller θ_v deficits within the forward flank of tornadic supercells when compared to nontornadic supercells. A later analysis at 0331 UTC (Fig. 4) displays observations closer to the hook echo and tornado. In this region of the storm, θ_v

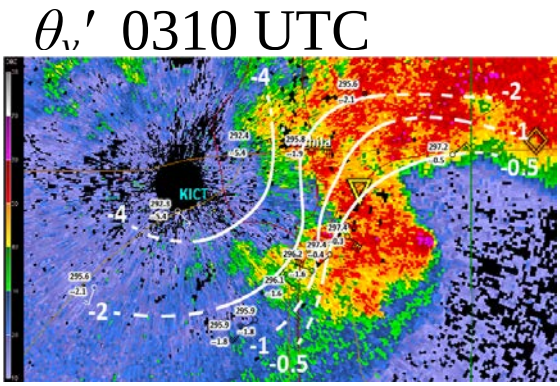

Figure 4. As in Fig. 3, only for 0331 UTC. The contour interval is 2 K, except that the -0.5 K and -1 K contours are also shown. In regions of high density surface observations, only every other observation is plotted for clarity.

deficits were similarly small, on the order of 0.5-2 K, which is in close agreement with Markowski et al. (2002).

The analysis of θ_e within the forward flank (Fig. 5), as well as within the rear flank (Fig. 6), also exhibit small deficits on the order of 3 K within the FFD, while the region of the RFD near the tornado contains deficits of 1-2 K. In the analysis conducted by Markowski et al. (2002) and Shabbott and Markowski (2006), θ_e deficits were typically less than 4 K within 2 km of the tornado, which closely matches the data analyzed in this case. These minimal deficits of θ_e and θ_v are likely related to greater surface-based buoyancy within the downdraft regions of this supercell, and hence greater likelihood of this air ascending through the updraft.

A region that has been sparsely observed in previous works is the left-rear flank of supercells, which in this case exhibits large deficits of θ_e and θ_v, on the order of 9 K and 5 K, respectively (Figs. 4 and 6). It is possible that these large deficits resulted from a separate downdraft (likely precipitation-driven) within the core of the storm. The thermodynamic analysis and low-level wind fields indicate that none of this cold air was feeding the tornado during the period in which it moved over the ASOS sites. Unfortunately, there are no surface observation sites farther northeast that may confirm whether or not this cold air ultimately flowed toward the tornado, and if this may have played a role in its dissipation.

A weak region of mesoscale high pressure with a maximum pressure greater than

θ_e' 0310 UTC

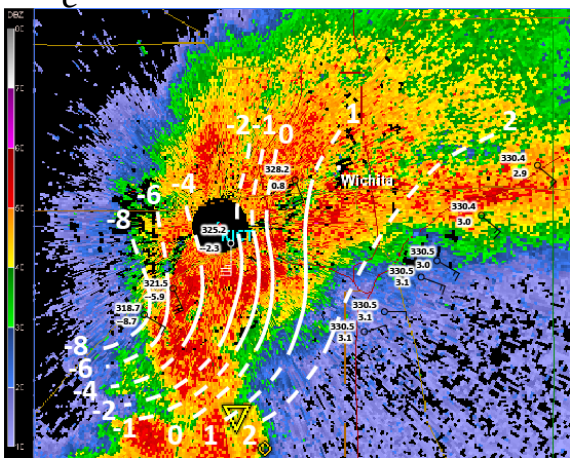

Figure 5. As in Fig. 3, only for θ_e at 0310 UTC. On the station models, the top number is θ_e (K) and the bottom number is θ_e' (K). Contour lines show θ_e', and the contour interval is 2 K, except that the -1 K and 1 K contours are also shown.

θ_e' 0331 UTC

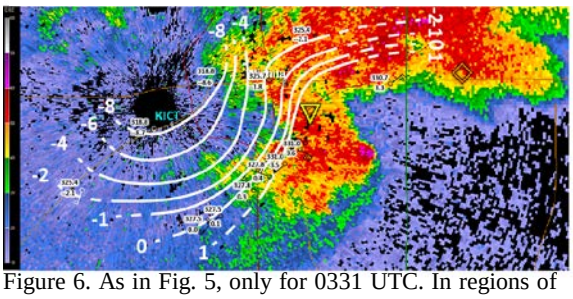

Figure 6. As in Fig. 5, only for 0331 UTC. In regions of high density surface observations, only every other observation is plotted for clarity.

1000 mb was observed within the forward-flank precipitation core (Fig. 7), as expected from modest low-level latent cooling. The area surrounding the tornado was characterized by low pressure; the minimum pressure observed at KIAB was 992.3 mb at 0333 UTC. At this time, the ASOS site was about 135 m from the edge of the tornado track, and was 915 m from the center of the tornado track (Figs. 1 and 8). The pressure deficit was almost 7 mb relative to the ambient environment at this time. It should be noted that this pressure deficit is significantly less than that observed in tornadoes in past work (e.g., Samaras 2004; Lee et al. 2004), but in this case, the sensor did not directly enter the tornado core flow region, and the data were of much coarser temporal resolution than that obtained by

p 0310 UTC

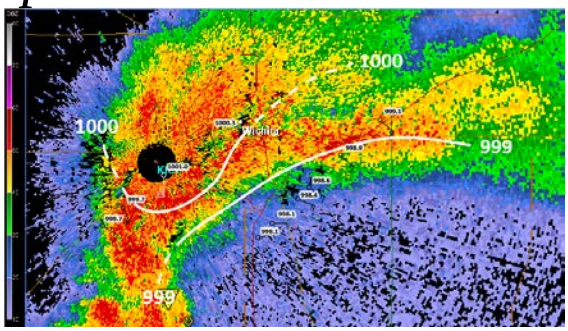

Figure 7. As in Fig 3, only for pressure (mb) at 0310 UTC. Contour interval is 1 mb.

p 0331 UTC

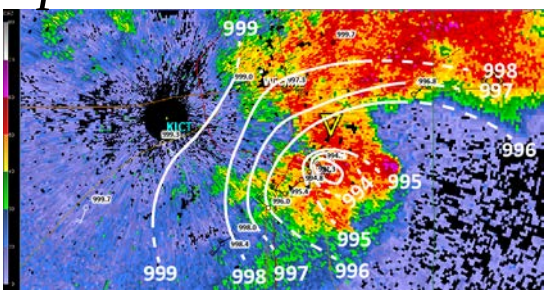

Figure 8. As in Fig. 7, only for 0331 UTC. In regions of high density surface observations, only every other observation is plotted for clarity.

specialized tornado research probes. Given that the horizontal pressure gradients within tornadoes have been previously observed to be up to 1 mb m^{-1} (Wurman and Samaras 2004), we do not expect this 7 mb pressure deficit to be representative of the pressure deficit within the center of the tornado.

One minute later, at 0334 UTC, KIAB observed a sustained wind speed of 48 knots (24.7 m s^{-1}) and a gust to 66 knots (34 m s^{-1}). The surface wind directions at this time do not seem to match with the low-level WSR-88D radial velocity field (Fig. 9). If a purely rotational wind field is assumed from the radar imagery, the winds at the KIAB ASOS site should be westerly. Instead, the observed wind direction is southwesterly. One possible reason for the discrepancy in wind directions is that the KICT radar beam was about 175 m above the surface observation site, so it is possible that the WSR-88D beam was above the inflow layer of the tornado, while the surface observation sampled the inflow layer. In the inflow layer,

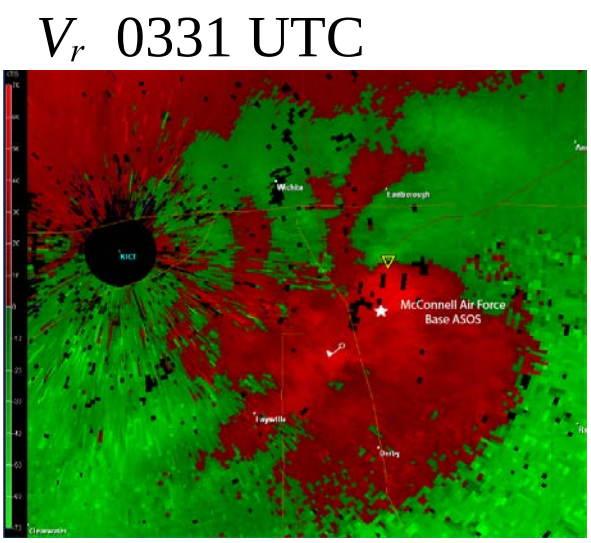

Figure 9. KICT radial velocity image at 0331 UTC. The wind observation at 0334 UTC is indicated after applying the time-to-space conversion. Location of the KIAB ASOS site is indicated by the white star.

winds not only rotate counter-clockwise, but also exhibit a radial component toward the tornado center, which would result in a surface wind from the southwest at the ASOS site.

4. Conclusions

High temporal resolution METAR observations from three ASOS sites, as well as WSR-88D radar data, allowed for a detailed analysis of the thermodynamic fields within this tornadic supercell. Analysis of θ_e and θ_v provide clear evidence which supplements the increasing understanding that relatively warmer and more potentially buoyant RFDs are associated with more long-lived and intense tornadoes. The minimum pressure measured was 992.3 mb, which represents a pressure deficit of 7 mb relative to the ambient environment about 915 meters from the center of the tornado. Surface wind observations near the tornado were consistent with inflow into the tornado below an altitude of 175 m.

It is apparent from this study that more such cases of both tornadic and nontornadic supercells moving in close proximity to surface observing sites should be analyzed in order to complement the existing surface observations from specialized field research projects such as The Verification of the Origins of Rotation in Tornadoes Experiment (VORTEX). The present analysis can be expanded to include calculations of surface-based convective available potential energy (CAPE) and convective inhibition (CIN), which would allow for a more in-depth examination of the surface-based buoyancy field surrounding the tornado. Storm-relative wind vectors should also be plotted and analyzed. This case also highlights the potential for future research in regard to the thermodynamic characteristics of the outflow on the left-rear flank of the storm, which in this case was found to exhibit large θ_e and θ_v deficits that differ greatly from the relatively small deficits seen closer to the tornado, and whose origins remain a mystery.

Acknowledgements. We are grateful to Zach Wienhoff for his assistance with image creation.

REFERENCES

Grzych, M. L., Lee, D. B., and Finley, C. A., 2007: Thermodynamic analysis of supercell rear-flank downdrafts from project ANSWERS. *Mon. Wea. Rev.*, **135**, 240–246.

Lee, B. D., Finley, C. A., and Samaras, T. M., 2011: Surface analysis near and within the Tipton, Kansas, tornado on 29 May 2008. *Mon. Wea. Rev.*, **139**, 370-386.

Lee, B. D., Finley, C. A., Karstens, C. D., 2012: The Bowdle, South Dakota, cyclic tornadic supercell of 22 May 2010: Surface analysis of rear-flank downdraft evolution and multiple internal surges. *Mon. Wea. Rev.*, in press.

Lee, J., T. Samaras, and C. Young, 2004: Pressure measurements at the ground in an EF-4 tornado. Preprints, *22nd Conf. on Severe Local Storms*, Amer. Meteor. Soc., Hyannis, MA, paper 15.3.

Markowski, P. M., Straka, J. M., Rasmussen, E. N., 2002: Direct surface thermodynamic observations within the rear-flank downdrafts of nontornadic and tornadic supercells. *Mon. Wea. Rev.*, **130**, 1692-1721.

National Weather Service, Wichita, Kansas, 2012: April 14th Tornado Outbreak. Available online: http://www.crh.noaa.gov/news/display_cmsstory.php?wfo=ict&storyid=81890&source=0 . Accessed 24 October 2012.

Samaras, T., 2004: A historical perspective of in-situ observations within tornado cores. Preprints, *22nd Conf. on Severe Local Storms*, Amer. Meteor. Soc., Hyannis, MA, paper P11.4.

Shabbott, C. J. and P. M. Markowski, 2006: Surface in situ observations within the outflow of forward-flank downdrafts of supercell thunderstorms. *Mon. Wea. Rev.*, **134**, 1422–1441.

Wurman, J. and Samaras, T., 2004: Comparison of in-situ pressure and DOW Doppler winds in a tornado and RHI vertical slices through 4 tornadoes during 1996-2004. Preprints, *22nd Conf. on Severe Local Storms*, Amer. Meteor. Soc., Hyannis, MA, paper 15.4.